



Automated quantification of spikes

Vamsidhar Chavakula^{a,b,1}, Iván Sánchez Fernández^{b,c,*}, Jurriaan M. Peters^{a,b}, Gautam Popli^d, William Bosl^a, Sanjay Rakhade^{a,b}, Alexander Rotenberg^{a,b}, Tobias Loddenkemper^{a,b}

^a Harvard Medical School, Boston, MA, USA

^b Division of Epilepsy and Clinical Neurophysiology, Department of Neurology, Boston Children's Hospital, Harvard Medical School, Boston, MA, USA

^c Department of Child Neurology, Hospital Sant Joan de Déu, Universidad de Barcelona, Barcelona, Spain

^d Wake Forest University Baptist Medical Center, Winston-Salem, NC, USA

ARTICLE INFO

Article history:

Received 11 July 2012

Revised 16 November 2012

Accepted 23 November 2012

Available online 3 January 2013

Keywords:

Automated quantification methods

Diagnosis

Electrical status epilepticus in sleep

Electroencephalography

Epilepsy

Sleep-wake cycle

Spikes

Spike detection

Spike focus lateralization

Wavelet transform

ABSTRACT

Methods for rapid and objective quantification of interictal spikes in raw, unprocessed electroencephalogram (EEG) samples are scarce. We evaluated the accuracy of a tailored automated spike quantification algorithm. The automated quantification was compared with the quantification by two board-certified clinical neurophysiologists (gold-standard) in five steps: 1) accuracy in a single EEG channel (5 EEG samples), 2) accuracy in multiple EEG channels and across different stages of the sleep-wake cycles (75 EEG samples), 3) capacity to detect lateralization of spikes (6 EEG samples), 4) accuracy after application of a machine-learning mechanism (11 EEG samples), and 5) accuracy during wakefulness only (8 EEG samples). Our method was accurate during all stages of the sleep-wake cycle and improved after the application of the machine-learning mechanism. Spikes were correctly lateralized in all cases. Our automated method was accurate in quantifying and detecting the lateralization of interictal spikes in raw unprocessed EEG samples.

© 2012 Elsevier Inc. All rights reserved.

1. Introduction

Electrical status epilepticus in sleep (ESES) is an electroencephalogram (EEG) pattern with a marked sleep potentiation of epileptiform activity in the transition from wakefulness to sleep that leads to near-continuous slow spikes and waves that occupy a significant proportion of non-REM sleep [1–3]. Patients with ESES demonstrate different degrees of cognitive regression [1–3], and several studies suggest that this regression is related to the continuous interictal spiking during sleep and that treatment of interictal spiking can potentially improve the cognitive outcome of patients with ESES [2–11]. However, there is no agreement as to how aggressively interictal spikes should be treated [12–15].

In part, this lack of consensus is due to a technical limitation: to answer whether interictal spiking correlates positively with a poor cognitive prognosis, investigators require a method to rapidly and objectively quantify spikes in a prolonged (sometimes lasting for several

days) EEG recording. Human quantification of interictal spikes is time-consuming, and intra- and inter-observer agreement is far from perfect [16–19]. In contrast to human performance, automatic algorithms are consistent, but their accuracy leaves room for improvement. Many of the much-needed automated algorithms for interpretation of the EEG have mainly focused on seizure detection [20–26]. A significant effort has also been made in order to develop algorithms that identify and quantify interictal spikes [27,28]. Spike detection protocols have traditionally relied on the detection of a series of template characteristics which limits their sensitivity to relatively stereotypical EEG spikes. In addition, most of those algorithms only yield good results when analyzing short and highly pre-processed EEG samples [27,28]. Therefore, algorithms that are insensitive to artifact and that objectively quantify interictal spikes of heterogeneous morphology are urgently needed.

In order to address this medical need, we developed a wavelet transform-based algorithm for the automatic quantification of spikes in raw unprocessed EEG samples. The objective of this study was to compare the quantification of spikes by the automatic algorithm with the quantification performed by two clinical neurophysiologists (gold-standard). Specifically, we aimed to 1) evaluate the algorithm's accuracy in quantifying spikes in a single channel, 2) test the consistency of this quantification in a multichannel EEG tracing across

* Corresponding author at: Division of Epilepsy and Clinical Neurophysiology, Fegan 9, Boston Children's Hospital, 300 Longwood Ave, Boston, MA 02115, USA. Fax: +1 617 730 0463.

E-mail address: ivan.fernandez@childrens.harvard.edu (I. Sánchez Fernández).

¹ The first two authors contributed equally to this manuscript.

different stages of the sleep-wake cycle, 3) assess the algorithm's capacity to detect lateralization of spikes in a multichannel EEG tracing, and 4) apply a computer-learning mechanism to refine the algorithm's accuracy.

2. Methods

2.1. Protocol approval and study design

This study was approved by the Institutional Review Board of Boston Children's Hospital. We performed a descriptive study on the performance of our algorithm for automated spike quantification. Our working hypothesis was that the performance of our automatic spike detection and quantification protocol will be similar to that of visual spike quantification by two epileptologists.

2.2. Spike quantification approach: our wavelet transform algorithm

The algorithm is intended to quantify spikes in raw EEG signals which have not been pre-processed, except for the omission of segments containing major artifact. We used a double threshold wavelet transform model, which provides a large initial encatchment for all possible spikes and then systematically pares down the contenders (Fig. 1 and Supplementary Fig. 1). Algorithm implementation was performed in Matlab R2009 (Mathworks, Natick, MA).

2.2.1. First round of analysis in an individual channel

We processed the raw EEG signal in order to extract the most useful information from it. In the first round of thresholding, wavelet decomposition was performed on the raw EEG signal (Figs. 1A and B), and the signal was transformed into a series of coefficients which was then automatically thresholded and used to reconstruct a new signal (Fig. 1C).

2.2.2. Second round of thresholding in an individual channel

In the second round of thresholding, we again obtained the mean and standard deviation of all points in the previous signal and classify the top 5th percentile of absolute values as spikes (Figs. 1D and E).

2.2.3. Adaptation of the wavelet algorithm for multichannel analysis

For the quantification of spikes in multiple channels, the algorithm was further refined with inter-channel comparison. Deflections that appeared only in one channel or simultaneously in all channels were considered as artifacts and were not quantified as spikes (Figs. 2A and B).

2.2.4. Adaptation of the method for detection of lateralization of spikes

To detect lateralization of spikes, the algorithm analyzed each EEG channel independently and calculated a spike area measurement for that channel, defined as the sum of the amplitudes of the spikes detected (Fig. 2C).

2.2.5. Implementation of machine-learning mechanism

To implement a machine learning-based classification system, at the spike timepoints marked by the wavelet transform module, the EEG was re-analyzed, and the amplitude, slope, and spike angle of each channel were recorded and used as defining features to train and classify a machine-learning algorithm.

2.3. Patients

We selected EEG samples from five patient groups.

2.3.1. Reliability in quantification of spikes in a single channel: Group I

2.3.1.1. Patients. We included all the patients (i) who were admitted for long-term video-EEG monitoring at our Epilepsy Unit, (ii) who

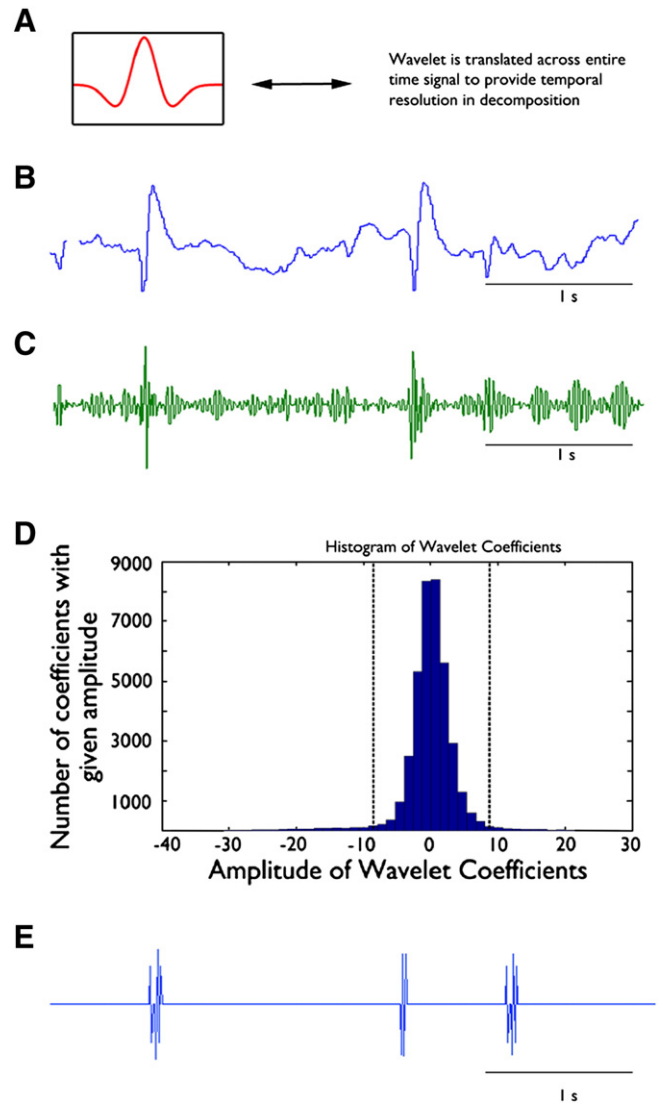


Fig. 1. Method of signal processing in our algorithm. A. A wavelet is a compact signal of finite length which serves as the basis of decomposition for a given signal. Frequency resolution is achieved by widening or contracting the signal while time resolution is achieved by translating it. B. Sample of the EEG recording to be analyzed. C. Output of the wavelet decomposition algorithm. It is evident that during large swings of the EEG recording, the output manifests large deflections in the decomposition signal, and this stands as the basis of our spike detection algorithm. D. A histogram of the wavelet decomposition coefficients. The middle 95% of values, lying in between the dashed vertical lines, will be thresholded to zero. E. A reconstruction of the potential spikes in the original signal.

were admitted during the period from January 1st, 2001 to December 31st, 2008, and (iii) who had a generalized ESES pattern with a least 80% of their non-REM sleep EEG occupied with spikes.

2.3.1.2. EEG segments. All patients underwent 24–96 h of continuous video-EEG monitoring, at 256-Hz sampling frequency. Scalp EEG electrodes were placed according to the 10–20 international system of electrode placement. For every patient, a segment of the first 300 s of non-REM sleep stage II (NREM II) was selected by two board-certified clinical neurophysiologists. From this segment, the channel with most frequent spikes (as evaluated by visual analysis) was selected for human and automated quantification.

2.3.1.3. Comparison of human and automated quantification. Spike quantification was performed by the application of the wavelet transform algorithm as well as by visual analysis by the two board-certified

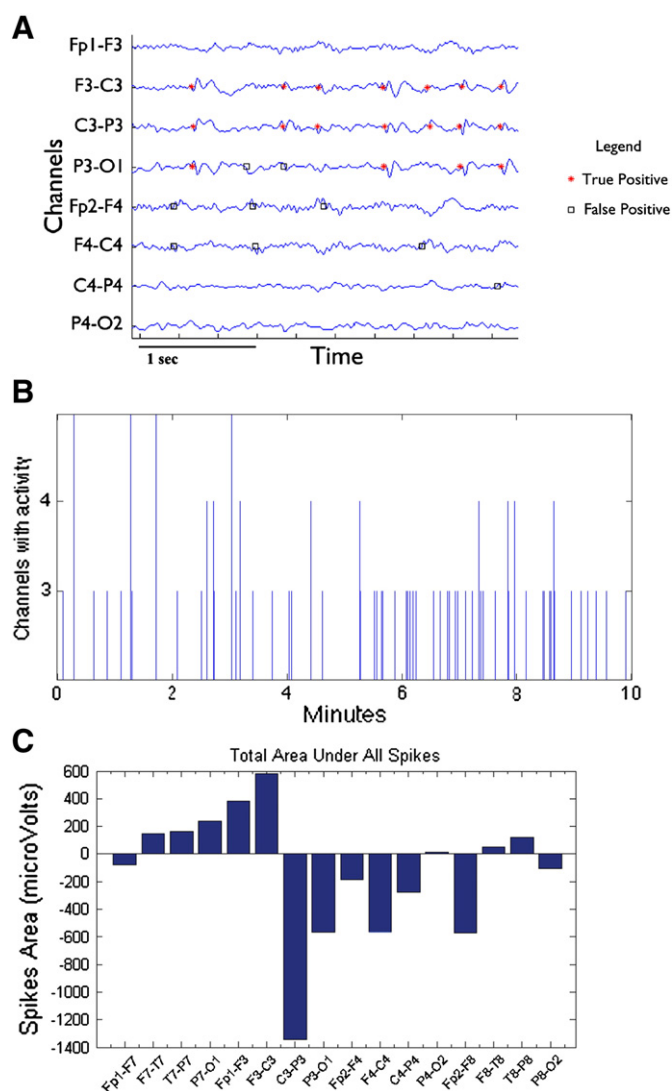


Fig. 2. A. Sample analysis of multichannel recording with spikes marked as true positives or false positives. B. Multichannel analysis with the number of channels with activity. C. Multichannel analysis as total spike area in each channel.

clinical neurophysiologists blinded to the results of the automated counting. Spike quantification was performed by calculating the spike frequency: number of spikes per 100 s. The samples were reviewed separately by two clinical electrophysiologists, and the mean was calculated. When a discrepancy of more than 10% in spike quantification was present, a third reviewer calculated the spikes, and the overall mean was calculated. These discrepancies, that occurred in less than 5% of tracings, were due to different interpretations of occasional EEG activity that presented features that could be interpreted as epileptiform or not epileptiform in nature. Performance was gauged by calculating the sensitivity and selectivity of the algorithm against the two reviewers.

2.3.2. Reliability in quantification of spikes across different stages of the sleep-wake cycle in a multichannel EEG tracing: Group II

2.3.2.1. Patients. We included all patients (i) who were admitted for long-term video-EEG monitoring at our Epilepsy Unit, (ii) who were admitted during the period from January 1st, 1995 to September 1st, 2010, and (iii) who had a generalized ESES pattern with a percentage of at least 50% of non-rapid eye movement (non-REM) sleep occupied by spike-waves, as stated in the clinical records.

2.3.2.2. EEG segments. All patients underwent 24–96 h of continuous video-EEG monitoring, at 256-Hz sampling frequency. Scalp EEG electrodes were placed according to the 10–20 international system of electrode placement. For every patient, three segments of one minute each in every overnight EEG tracing were selected by experienced board-certified clinical neurophysiologists: (1) the first clearly recognizable segment of wakefulness, (2) the first clearly recognizable segment of NREM2 sleep, and (3) the first clearly recognizable segment of NREM3 sleep.

2.3.2.3. Comparison of human and automated quantification. The two board-certified clinical neurophysiologists, blinded to the results of the automated counting, calculated the spike-wave percentage (SWP) as the percentage of one-second bins occupied by, at least, one spike-wave and “human” spike frequency (hSF) as the total number of spikes per 100 s. The samples were reviewed separately by the two reviewers, and the mean was calculated. When a discrepancy of more than 10% in spike quantification was present, a third reviewer calculated the spikes, and the overall mean was calculated. On the same EEG tracings, the algorithm calculated “automated” spike frequency (aSF).

2.3.3. Lateralization of spikes in a multichannel EEG tracing: Group III

2.3.3.1. Patients. We included all patients (i) who had an ambulatory EEG recording performed at our Epilepsy Unit (ii) who were admitted during the period from January 1st, 2009 to December 31st, 2009, and (iii) who had a clinical presentation compatible with ‘benign’ childhood epilepsy with centro-temporal spikes (BECTS) with unilateral continuous spike-waves compatible with a unilateral ESES tracing.

2.3.3.2. EEG segments. All patients underwent at least 24 h of continuous EEG monitoring, at 512-Hz sampling frequency. Scalp EEG electrodes were placed according to the 10–20 international system of electrode placement. Between 8 min and 12 min of continuous recordings without major artifacts were selected from each recording by board-certified clinical neurophysiologists.

2.3.3.3. Comparison of human and automated quantification. Spike quantification was performed by the application of the wavelet transform algorithm as well as by visual analysis by two experienced board-certified clinical neurophysiologists. Spike quantification was performed by calculating the spike frequency: total number of spikes per 100 s. The two reviewers agreed on their evaluation in all cases. Spikes were considered to be lateralized to a given hemisphere when the spike area or spike quantification of over 50% of the channels of a given hemisphere was greater than the spike area or spike quantification of the contralateral hemisphere.

2.3.4. Addition of machine learning component: Group IV

2.3.4.1. Patients. We included all the patients (i) who were admitted for long-term video-EEG monitoring at our Epilepsy Unit, (ii) who were admitted during the period from January 1st, 2001 to December 31st, 2008, and (iii) who had a generalized electrical status epilepticus in sleep (ESES) pattern with at least 50% of their non-REM sleep EEG occupied with spikes.

2.3.4.2. EEG segments. All patients underwent 24–96 h of continuous video-EEG monitoring, at 256-Hz sampling frequency. Scalp EEG electrodes were placed according to the 10–20 international system of electrode placement. For every patient, a segment of three- to eight-minute duration of non-REM sleep stage II (NREM II) was selected by two board-certified clinical neurophysiologists.

2.3.4.3. Spike algorithm. Each recording was first analyzed using a double threshold wavelet method to highlight time points corresponding to potential spike events. For each detected spike, the amplitude, slope, and spike angle in every channel were calculated. These features were inserted into a machine-learning algorithm to determine whether the time point was indeed a spike. Machine-learning classifier training and testing for each set were performed using a 10-fold cross-validation technique.

2.3.4.4. Comparison of human and automated quantification. Spike quantification was performed by the application of the wavelet transform/machine learning algorithm. Afterward, the results were compared with the visual quantitative analysis by two board-certified clinical neurophysiologists.

2.3.5. Detection of interictal spikes during wakefulness: Group V

2.3.5.1. Patients. In order to evaluate how the algorithm behaves during wakefulness, a period with a lower signal-to-noise ratio (eye blinks, muscle, and other artifacts), we included consecutive patients (i) who underwent an EEG at our Epilepsy Unit, (ii) who were admitted during the period from January 2012 to September 2012, and (iii) who had frequent (at least 40%) interictal epileptiform discharges during wakefulness.

2.3.5.2. EEG segments. All patients underwent video-EEG of different durations, at 256-Hz sampling frequency. Scalp EEG electrodes were placed according to the 10–20 international system of electrode placement. For every patient, the first available segment of five-minute duration of wakefulness was collected.

2.3.5.3. Spike algorithm. Each recording was first analyzed using a double threshold wavelet method to highlight time points corresponding to potential spike events. For each detected spike, the amplitude, slope, and spike angle in every channel were calculated. These features were inserted into a machine learning algorithm to determine whether the time point was indeed a spike. Machine-learning classifier training and testing for each set were performed using a 10-fold cross-validation technique.

2.3.5.4. Comparison of human and automated quantification. Spike quantification was performed by the application of the wavelet transform/machine-learning algorithm. Subsequently the results were compared with the visual quantitative analysis by two board-certified clinical neurophysiologists.

2.4. Statistical analysis

We evaluated the relationship between human and automated quantification using the Pearson correlation coefficient. All analyses were performed using SPSS 19 (SPSS Inc., Chicago, IL).

3. Results

3.1. Reliability in quantification of spikes in a single channel: Group I

3.1.1. Patients and EEG segments

Five patients with one EEG segment each were included in the analysis. Their demographic and clinical characteristics can be found in Supplementary Table 1.

3.1.2. Comparison of human and automated quantification

Our algorithm detected 882 of the 1231 spikes marked by the human reviewers, yielding a sensitivity of 72% (range: 53% to 90%). Our algorithm detected 882 true spikes and 496 false spikes (spikes not detected by the human reviewer), yielding a selectivity of 64%.

The total number of spikes detected by the algorithm and the number of human marked spikes correlated ($R = 0.35$, $p < 0.0001$).

3.2. Reliability in quantification of spikes across different stages of the sleep-wake cycle in a multichannel EEG tracing: Group II

3.2.1. Patients and EEG segments

Twenty-five patients with three EEG segments each (75 EEG segments in total) were included in the analysis. Their demographic and clinical characteristics can be found in Supplementary Table 2.

3.2.2. Comparison of human and automated quantification

Spikes calculated with the automated and human quantification were highly correlated in all stages of the sleep-wake cycle (Table 1).

3.3. Lateralization of spikes in a multichannel EEG tracing: Group III

3.3.1. Patients and EEG segments

Six patients with one EEG segment each were included in the analysis. Their demographic and clinical characteristics can be found in Supplementary Table 3.

3.3.2. Comparison of human and automated quantification

Automated analysis was able to localize 100% of the discharges to the correct side. Regarding reliability of spike quantification, our algorithm detected 1836 out of 2409 spikes marked by the human reviewer, yielding an overall sensitivity of 76% (range: 62% to 91%).

3.4. Addition of machine-learning component: Group IV

3.4.1. Patients and EEG segments

Eleven patients with one EEG segment each were included in the analysis. Their demographic and clinical characteristics can be found in Supplementary Table 4.

3.4.2. Comparison of human and automated quantification

Two different machine-learning modalities were tested—support vector machine (SVM) and Bayesian learning. When SVM was used, the overall sensitivity was 69.6% (+/− 15.3%), and the overall specificity was 95.7% (+/− 10.4%). The kappa statistic values were 0.878 and 0.854 respectively for reviewers A and B. When Bayesian learning was utilized, the overall sensitivity was 77.6% (+/− 9.1%), and the overall specificity was 87.6% (+/− 8.3%), and the kappa statistic values were 0.780 and 0.771 respectively for reviewers A and B. The detailed results are provided in Table 2. The trade-off encountered between algorithm sensitivity and specificity is presented in the ROC curve in Fig. 3.

Table 1

Correlation of the automated and human methods of spike quantification in Group II.

| | hSF-W | hSF-II | hSF-III | aSF-W | aSF-II | aSF-III |
|---------|----------------------------|----------------------------|----------------------------|----------------------------|---------------------------|---------------------------|
| SWP-W | R = 0.967; $p < 0.0001$ | | | R = 0.588; $p = 0.002$ | | |
| SWP-II | | R = 0.871; $p < 0.0001$ | | | R = 0.434; $p = 0.03$ | |
| SWP-III | | | R = 0.898; $p < 0.0001$ | | | R = 0.494; $p = 0.012$ |
| SF-W | | | | R = 0.652; $p < 0.0001$ | | |
| SF-II | | | | | R = 0.575; $p = 0.003$ | |
| SF-III | | | | | | R = 0.484; $p = 0.014$ |

aSF: automated spike frequency. hSF: human spike frequency. SWP: spike-wave percentage. W: wakefulness. II: non-REM sleep II. III: non-REM sleep III. R: Pearson correlation coefficient.

Table 2
Correlation of the automated and human methods of spike quantification in Group IV.

| Set | SVM | | Bayes | |
|---------|-------------|-------------|-------------|-------------|
| | Sensitivity | Specificity | Sensitivity | Specificity |
| 1 | 0.844 | 0.622 | 0.816 | 0.693 |
| 2 | 0.864 | 0.980 | 0.864 | 0.896 |
| 3 | 0.729 | 0.967 | 0.785 | 0.890 |
| 4 | 0.724 | 0.969 | 0.796 | 0.923 |
| 5 | 0.474 | 0.975 | 0.720 | 0.913 |
| 6 | 0.692 | 0.971 | 0.820 | 0.929 |
| 7 | 0.828 | 0.887 | 0.611 | 0.792 |
| 8 | 0.685 | 0.977 | 0.861 | 0.936 |
| 9 | 0.845 | 0.953 | 0.950 | 0.893 |
| 10 | 0.465 | 0.938 | 0.746 | 0.763 |
| 11 | 0.499 | 0.953 | 0.717 | 0.784 |
| Overall | 0.696 | 0.957 | 0.776 | 0.876 |

SVM: support vector machine.

3.5. Detection of interictal spikes during wakefulness: Group V

3.5.1. Patients and EEG segments

Eight patients with an EEG segment of at least five-minutes duration each were included in the analysis. Their demographic and clinical characteristics can be found in Supplementary Table 5.

3.5.2. Comparison of human and automated quantification

The kappa correlation coefficient of the two human reviewers for this set of EEG tracings was 0.77. The algorithm for the four EEG tracings with moderate artifact (Supplementary Fig. 2A) demonstrated a sensitivity of 0.75, a specificity of 0.82, and an area under the curve of 0.86. The algorithm for the four EEG tracings with prominent muscle artifact (Supplementary Fig. 2B) demonstrated a sensitivity of 0.43, a specificity of 0.89, and an area under the curve of 0.81 (Table 3).

4. Discussion

Our data demonstrate that our wavelet transform algorithm is accurate for quantification of spikes across all stages of the sleep-wake

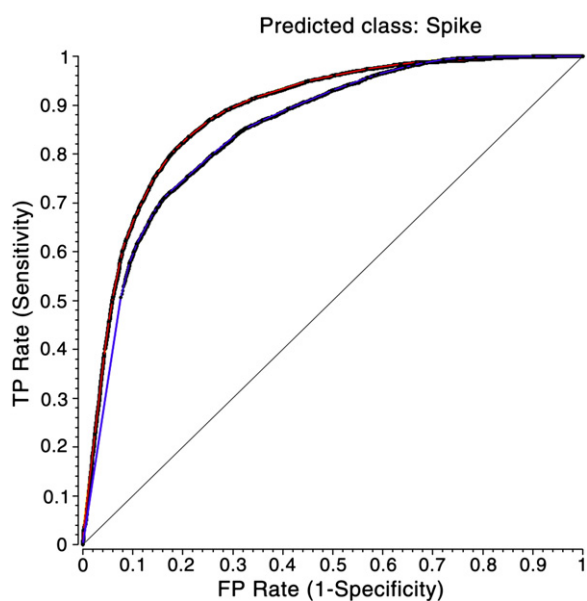


Fig. 3. Receiver–operator characteristic curve shows the relation of sensitivity and specificity in our algorithm when compared with the gold-standard human reviewer. Two methods are used: support vector machine (red line) and Bayesian learning (blue line).

Table 3
Correlation of the automated quantification method to the human reviewers' quantification during wakefulness in Group V.

| | Set | Human reviewer 1 | | Human reviewer 2 | |
|---------------------------|-----|------------------|-------------|------------------|-------------|
| | | Sensitivity | Specificity | Sensitivity | Specificity |
| Moderate muscle artifact | 1 | 0.641 | 0.772 | 0.814 | 0.693 |
| | 2 | 0.727 | 0.872 | 0.739 | 0.902 |
| | 3 | 0.794 | 0.897 | 0.797 | 0.895 |
| | 4 | 0.714 | 0.762 | 0.732 | 0.774 |
| Prominent muscle artifact | 5 | 0.387 | 0.968 | 0.411 | 0.967 |
| | 6 | 0.609 | 0.854 | 0.564 | 0.896 |
| | 7 | 0.482 | 0.788 | 0.48 | 0.821 |
| | 8 | 0.324 | 0.89 | 0.22 | 0.956 |

cycle and correctly detects lateralization of spikes. A major advantage of our algorithm is that it does not require prior human processing of the EEG in order to recognize spikes.

4.1. Detection of spikes

Methods of spike recognition have evolved from detection of EEG morphologies similar to pre-established template spikes, to complex signal processing methods with analysis of decomposed EEG elements.

4.1.1. Template matching

The earliest methods of automated EEG quantification were based on the calculation of cross-correlations of EEG elements with template spikes. When this cross-correlation exceeded a certain arbitrary threshold, the element was classified as a spike [29].

4.1.2. Mimetic analysis

A more refined version of the method above relies on recognition of segments of EEG situated between areas of extreme amplitude. These waves are divided into half-waves in which duration, amplitude, slope, sharpness, and emergence from the background are analyzed [30,31]. The primary concern with both these methods is that true events may not match the prototypical description sufficiently and will not be recognized. Our wavelet transform algorithm is able to automatically alter its frequency and time resolution in order to recognize a wide variability of spike morphologies (Fig. 1).

4.1.3. Fourier transform

Spectral analysis quantifies the power in a pre-specified number of frequency bands. Power spectrum measures can be useful for the detection of high-frequency oscillations [32] or standard, relatively uniform, spikes [33]. The most common type of power spectral analysis used in spike quantification is the Fourier transform. However, this approach is limited because it possesses poor temporal resolution, and any attempt to increase the resolution in time decreases the resolution in frequency and vice versa. The wavelet transform algorithm stands out because it can perform frequency analysis while maintaining temporal resolution. In fact, our algorithm can modify its temporal resolution to the individual tracing (Fig. 1).

4.1.4. Machine-learning algorithms

Artificial neural networks rely on training a network with a dataset of features considered to be true spikes as compared with features deemed to be non-spikes [34]. The major concern with this approach is that a neural network is only as comprehensive as its training dataset. Hence, if a neural network has not been trained with a certain pattern, it will not be able to recognize that pattern in subsequent analysis. The wavelet transform analyzes the features of a spike without previous training. However, because of the capacity to intrinsically

modify frequency and time resolution, our algorithm is able to recognize the basic features of a spike even if never exposed to it. Our algorithm demonstrates that it can recognize basic spike features even without prior training and that a machine-learning module may be easily added in order to provide improved spike detection with smaller training sets than other methods.

4.1.5. Wavelet transform

In our implementation of the wavelet transform, high-frequency components of the EEG are analyzed with a more precise time resolution than low-frequency components. This property is desirable, especially when analyzing fast transient waveforms, such as EEG spikes [35]. The original application of wavelets for the detection of spike-waves relied on highly pre-processed and very short EEG segments (5.12 s) with or without spike-waves in these segments. The algorithm was required to provide a binary answer to the question: are there spike-waves in this EEG segment? [35]. While this method allowed for the straightforward calculation of true positives, true negatives, false positives, and false negatives and the related sensitivity and specificity, it did not analyze raw EEG data [35]. A more realistic approach to the analysis of raw EEG data implies that true negatives are difficult to define and calculate: most of the EEG will not have spikes, and, therefore, true negatives tend to be infinite, and specificity tends to be 100% regardless of the actual performance of the algorithm. Thus, methods which analyzed long segments of raw EEG were more likely to report efficacy measures than specificity (Table 4).

Previous methods that were based on the wavelet transform have utilized a multilevel wavelet decomposition with single threshold of coefficients to isolate spikes [36]. The wavelet coefficients can also be used to determine the rhythmicity and energy of a signal in order to detect the repetitive rhythmicity of similar waves typical in a seizure [26,37]. All previous algorithms depended on training with a specific EEG tracing, and the detection capacity is limited to the patterns that the algorithm was exposed to during training. Our algorithm possessed the capacity to recognize spikes without prior training.

Algorithms using a wavelet transform and a neural network analysis represented the background for our study [35,38]. These algorithms required highly pre-processed EEG samples of very short duration (up to 15 s) in which spikes were either present or absent. In these studies, the algorithm was also required to answer a binary question about the presence or absence of a spike in the segment. In contrast, our algorithm was given a raw EEG and had to determine the localization of the spikes in a long segment while distinguishing it from similar graphoelements and artifacts. In a study of prolonged EEG segments of raw EEG (without using a neural network analysis), the agreement of the human and automated detection was merely 24–32% [39]. Therefore, our algorithm outperforms previous algorithms in detection and quantification of epileptiform activity in long unprocessed EEG segments. During the development of the binary algorithms (presence or absence of epileptiform activity in a very short segment of highly processed EEG), the progressive automatization of the selection of parameters in this study provided progressively better results from those of [35] and [38]. The difficulty in applying this method to long segments of unprocessed EEG was due to the need of a series of pre-established features of the spikes to be recognized leading to the need of a training phase. We have overcome this limitation by using an automated process of several levels of thresholding. Therefore the current algorithm does not require any pre-established spike features.

4.2. Quantification of spikes (Table 4)

Many methods of automated analysis of the EEG have focused on detecting seizures, by identifying patterns of repeated waves of similar morphology [20–26]. Methods focused on quantifying interictal

spikes have various weaknesses [39–42]. The most primitive application of the wavelet analysis defined the thresholds based on previous human experience [39]. Several other approaches all required training of the algorithm in order to detect the typical spikes [36,38,40,41]. Another algorithm was able to recognize typical spikes by itself but did not take into account the possibility of different shapes of spikes in the same patient [42]. Success with these approaches has been modest [39], moderate [41], or high [38,40,42]. However, analysis of raw EEG data yielded poor results [39]. Better results were obtained with EEG samples with stereotypical spikes [40–42] without testing heterogeneous spikes. In summary, approaches based on wavelet analysis as the main component [36] or as part of a more complex algorithm [38] and algorithms using alternative approaches such as independent component analysis [43] can yield good results, but they require a training phase and/or pre-processing of the EEG data. Our algorithm was able to modify its time and frequency resolutions in order to provide flexibility in the recognition of heterogeneous spikes in raw EEG data. In fact, our algorithm proved to be accurate in five sets of different patients, with two different EEG presentations: bilateral and unilateral ESES and during all stages of the sleep-wake cycle. The addition of a machine-learning component to the wavelet algorithm allowed for custom tailoring of spike feature detection to the individual patient in order to provide the optimal sensitivity and specificity.

4.3. Clinical relevance and outlook

Automated wavelet-based spike detection and quantification algorithms lend themselves to real-time calculation by a computational device. We envision implementation of this algorithm in an embedded hardware device, which could instantly detect spikes during EEG recordings in real time, as well as identify localized time periods during which abnormal spike patterns are detected. The development of a method for reliable quantification of spikes would be a first step in understanding the relevance of interictal spikes in cognitive regression [44–48]. Our algorithm is intended to provide quantification of spikes in all types of epilepsy syndromes. However, it was mainly tested in patients with ESES because of two reasons. First, patients with ESES present frequent spikes in their non-REM EEG tracing and, therefore, provide a tracing that is particularly rich of testing points (spikes), seldom present in other epileptic syndromes. Second, the amount of interictal spikes in ESES has been proposed as a significant causal mechanism in the neurocognitive regression of patients with ESES [46,47,49,50]. However, quantification of the epileptiform activity is limited because the comprehensive spike marking required for this type of study is too time-consuming for visual identification by clinical electrophysiologists [28]. This has impeded the development of studies on the correlation between amount of epileptiform activity and neurocognitive regression in ESES. The results of our algorithm may have an immediate implication in clinical practice as they will allow us to correlate this quantification of spikes with the clinical features of patients with ESES. In addition, our algorithm provided good results in patients with different epileptic syndromes (Group V).

Additionally, our algorithm would allow the implementation of a closed loop treatment strategy that would tailor treatment to the specific patient needs in every period of the disease [51].

4.4. Strengths and weaknesses

Our results need to be interpreted in the setting of data acquisition. Because the study was performed at a tertiary referral center, pediatric hospital, the study subjects may not be representative of the general population of patients with ESES. However, the purpose of our study was to compare the quantification of spikes with the automated algorithm with that of the human reader (gold-standard), and results

Table 4
Comparison of spike detection algorithms.

| | Method | Strengths | Weaknesses | Patient population | Training phase required | Analysis of raw prolonged EEG data | Measures of efficacy | Stages of the sleep-wake cycle included in the study |
|--------------------------|---|---|---|--|--|------------------------------------|--|---|
| Kalayci and Ozdamar [35] | Wavelet transform and neuronal networks training and testing | Use of both wavelet transform and neuronal networks | The EEG data were highly pre-processed with the selection of very short segments (5.12 second duration) with or without spikes in them Training set and testing set from the same patients | EEG data from 5 patients diagnosed with epilepsy | Yes | No | Variable accuracy depending on the scales with a maximum of 91.4% | Not specified |
| Dümpelmann et al. [39] | Wavelet analysis Comparison of the EEG signal with the background and pre-defined values of amplitude and duration | Use of both mimetic analysis and wavelet analysis | Parameters and thresholds had to be pre-set based on human experience | A total of 136 min of intracranial EEG from 7 patients | No | Yes | Agreement between automatic detection and human detection: 24%–32% | Not specified |
| Argoud et al. [38] | Multiple steps to analyze the EEG data | Integration of wavelet transform and neuronal networks in the same algorithm | Different results depending on different thresholds Trained on one standard set of features classification Cannot personalize analysis to individual patient | Nine long-term recordings from 7 patients with epilepsy The data analyzed were ten 15-second segments randomly selected from each patient | Yes | No | Sensitivity = 70.9% Specificity = 99.9% | Different stages of the sleep-wake cycle ^a |
| De Lucia et al. [43] | Independent component analysis | Two stages of spike detection | Requires pre-processing and training | 7 patients with epileptiform activity | Yes | No | Sensitivity = 65% Specificity = 86% | Unspecified |
| Larsson et al. [41] | Template matching | Controlled and well understood spike matching technique | Cannot perform multi-morphology multifoci analysis | “Approximately 200 patients with ESES” | Yes (from the same patient) | No | “Almost linear relation between number of spikes and spike index” | Sleep only |
| Nonclercq et al. [42] | Template matching | Multistage matching to enhance sensitivity | It is based on homogeneous spike morphology | First study: 3 children with CSWS Second study: 11 children with CSWS | No | No | Average spike-wave index estimation error First study: 5% SWI error Second study: 4.4% SWI error | First study: all stages ^a Second study: non-REM stages I and II |
| Indiradevi et al. [36] | Two-level wavelet analysis | No previous training required | Ignored positive deflection spikes | 22 patients with epilepsy | Yes | No | Sensitivity = 91.7% Specificity = 89.3% Selectivity = 78.1% Accuracy = 90.5% PPV = 92% Sensitivity = 82% | Not specified |
| Adjouadi et al. [40] | Walsh transform | Automatically discard artifact | Need for meeting many criteria (can overlook spikes with atypical features) | 31 patients with focal epilepsy (10 for training phase and 21 for analysis) | Yes (patients with the same type of epilepsy) | No | | All stages ^a |
| Present algorithm | Wavelet transform machine learning | Extracts multiple spike morphologies at multiple foci to provide localization | Presence of false positives | Group I: 5 patients with ESES Group II: 25 patients with ESES Group III: 6 patients with BECTS Group IV: 11 patients with ESES Group V: 8 patients with drug-refractory epilepsy and frequent interictal discharges during the day | Yes, if machine learning component implemented | Yes | Group I: Sensitivity = 72% Selectivity = 64% Group II: R = > 0.4 in all stages of the sleep wakefulness cycle Group III: 100% correct lateralization of spikes Group IV: Sensitivity = 70–78% Specificity = 88–96% Group V: Sensitivity = 0.43–0.75 Specificity = 0.82–0.89 | Group I: non-REM stage II Group II: all stages ^b Group III: non-REM sleep Group IV: non-REM sleep Group V: wakefulness |

BECTS: 'benign' focal epilepsy with centro-temporal spikes. ESES: electrical status epilepticus in sleep. PPV: positive predictive value. R = Pearson correlation coefficient.

^a Performance of the algorithm was not compared across different stages of the wake/sleep cycle.

^b Performance of the algorithm was compared across different stages of the wake/sleep cycle.

should not be influenced by the severity of the ESES pattern. Different clinical neurophysiologists interpreted the EEG, which may have led to inter-observer variability, yet it clearly demonstrates that our algorithm overcomes this subjectivity and correlates with all readers' visual assessments. A major strength of our study is that it demonstrates that algorithm performed consistently well, regardless among individual human readers, different stages of the sleep-wake cycle, and different electro-clinical conditions.

The manual counting by a human reviewer and the automated counting by our algorithm were compared in every one of the four steps of our study. Similarly, the measures such as sensitivity and false detection were applied to all of the steps in our study. One reason why different accuracy measures were necessary has to do with the ambiguous definition of a true negative spike. Some methods rely on a "bin method" whereby the EEG segment is divided into epochs of a given length, and each bin is classified by both human and computer, to definitively determine whether a bin segment was a true positive, true negative, false positive, or false negative spike. However, such a method may be viewed as artificial in that human reviewers do not normally analyze a recording as a series of strictly defined bins. In tests I–III, we allowed the visual reviewer the freedom to mark spikes as they normally would when reading an EEG recording. This meant that we were unable to define clearly true negative spikes. In test IV, we were able to exploit the two-stage algorithm in order to define true negatives. The output of the wavelet processing section of the algorithm yields a large number of candidate spikes, and cross-comparison of these spikes against human spikes allowed us to create a pool of spikes classified as true/false positives and true/false negatives. By passing these spike data through the machine-learning classifier component, we could then compare the final algorithm classification of various candidate spikes against their preliminary classification. Specificity and selectivity were decreased by false positive spike detection due to noise and artifact. At this time, we have developed our algorithm to have adequate sensitivity but at the cost of false positives. With the addition of a machine-learning component, we were able to overcome this challenge and boost specificity to greater than 95%. The learning algorithm did perform with less efficacy in the patients with multifocal spikes. However, in these cases, only the sensitivity was affected, while specificity was still quite high.

Two considerations should be taken into account when evaluating our results: 1) while previous studies required significant human intervention before the data were interpreted by the algorithm [40–42], our EEG data were raw EEG segments that were automatically interpreted by the algorithm without prior pre-processing, and 2) human quantification is not perfect, that is, human quantification may also include variability; two experts often do not mark the same events as spikes [16–19]; therefore, sensitivities and specificities around 80–90% may be considered in the upper limit of performance of any automated detection method that is compared with the human "gold-standard".

The sample size of each test was different because each specific question dictated the inclusion criteria of the patient sample studied. The test in Group I was an exploratory evaluation of the ability of the algorithm to detect spikes, and a large number of testing points was preferred. Therefore, patients with very frequent spikes required a spike threshold of 80%. The test in Group II aimed to evaluate the performance of the algorithm in different stages of the sleep-wake cycle; thus, inclusion was limited by the availability of EEG tracings with different stages of sleep and wakefulness, and patients with a lower threshold of 50% were included. Group III consisted of patients with clearly lateralized spikes to evaluate the capacity to detect lateralization of epileptiform activity. The tests in Group IV required longer duration of EEG samples, which was the limiting factor for recruitment. The tests in Group V required patients with frequent interictal spiking during wakefulness. Inclusion and exclusion criteria were tailored to

obtain a sample that would answer the specific question of each test. Therefore, the application of all approaches to all samples would not have answered additional questions. Furthermore, the differences in the length of the EEG samples in the different tests did not allow the use of the machine-learning algorithm for all of them.

It can be argued that the localization of the lateralization of epileptiform activity in EEG tracings with unilateral epileptiform activity is of limited practical relevance. However, such an analysis has not been done with prior automated algorithms and we aimed to demonstrate its feasibility; our algorithm localized the lateralization of epileptiform activity to the correct side in 100% of cases. A refined algorithm able to automatically detect the predominant lateralization in EEG segments with subtle lateralized epileptiform activity is under development. This refined algorithm will be capable of providing lateralization information in long segments of EEG in which lateralization may be difficult to detect by the human reviewer.

The data of the machine learning component were based on the analysis of 11 segments of 3–8 min of duration from 11 different patients and 8 segments of 5–6 min of duration from 8 different patients. Comparable previous work analyzed prolonged raw EEG data, using a total of 136 min from 7 patients [39]. A multistep analysis of the EEG used ten 15-second segments from 7 different patients [38]. The population of patients in Groups IV and V is, therefore, the largest among comparable studies and similar to studies with other approaches (Table 4). Even if contamination with artifacts in stage II sleep was low, sleep graphoelements (such as vertex waves, sleep spindles, or K-complexes) could have been confused with spikes. We purposefully applied our algorithm to EEG segments with certain distinct features to test its ability to clearly detect certain characteristics in multiple settings. Having assessed its performance in various domains of EEG analysis, we plan to apply it in non-selected EEG samples. Overall, the present study required a lesser amount of pre-processing than the previously reported studies [35,36,38,40–43].

Our original algorithm (the one used in the first three sets of patients) did not rely on a number of pre-set morphologies of the spikes but filtered the different signals in the EEG tracing in order to recognize those elements that stood out of the baseline. When the machine-learning algorithm was added to the original algorithm (the one used in the fourth and fifth sets of patients), our algorithm became self-adaptive because it was able to adapt in order to recognize the particular features that make a spike in a particular EEG tracing based on the baseline characteristics of the spikes in that particular EEG tracing. A major advantage of our algorithm is that we can alter analysis by training on the individual patient when necessary.

It can be argued that in an EEG tracing with infrequent interictal spikes and frequent eye blinking and muscle artifact during wakefulness, the signal-to-noise ratio would be lower, and the performance of our algorithm would decrease. However, the performance of our algorithm was tested during wakefulness in 25 one-minute EEG samples from 25 different patients in Group II. The performance was found to correlate moderately for automated spike frequency with human spike frequency and for automated spike frequency with human spike-wave percentage, as shown in Table 1. In addition, in order to evaluate specifically how the algorithm behaves during EEG tracings during wakefulness, a period with a lower signal-to-noise ratio (eye blinks, muscle artifact, etc.), we included eight consecutive patients with moderate to prominent noise (eye blinks, muscle artifact, etc.) (Supplementary Figs. 2A and 2B). Our algorithm remained accurate, especially in the group of patients with moderate muscle artifact. Further development of our algorithm will allow the correction for very prominent muscle artifact (Supplementary Fig. 2B). Therefore, our algorithm has been shown to perform moderately well during a long period (25 min in total from 25 different patients plus more than 40 min from 8 different patients) of wakefulness, where a lower amount of spikes is present and the signal-to-noise ratio is lower.

We agree with the comment brought up in the study by Wilson and Emerson in 2002 that the amount of EEG studied in present literature on automated detection is smaller than the training of human epileptologists: “Compare these values with those seen by a clinical neurophysiologist over the course of a year: about 100 patients, 10,000 spikes (200 spikes/week) and 800 h of EEG (8 h of detailed review/patient). We will probably not see expert-level algorithms until this amount of data is used for algorithm training” [28]. Performing this amount of EEG selection and analysis will require a larger study to select the appropriate amount of EEG data. Our study expands available literature (Table 4): 1) EEG samples are analyzed from many different perspectives in order to address different aspects of automated EEG analysis, 2) the number and length of the analyzed EEG samples are, at least, similar and, in most instances, larger than in previous studies, and 3) the performance of the automated detection algorithm is compared during different stages of the wake/sleep cycle.

5. Conclusion

Our wavelet transform algorithm for quantification of spikes demonstrated accuracy across all stages of the sleep-wake cycle and correctly detected lateralization of spikes. In addition, its performance was improved by a machine-learning mechanism.

Supplementary data to this article can be found online at <http://dx.doi.org/10.1016/j.yebeh.2012.11.048>.

Acknowledgments

Iván Sánchez Fernández is funded by a grant for the study of Epileptic Encephalopathies from “Fundación Alfonso Martín Escudero”.

Jurriaan Peters is funded by the NIH/NINDS (P20 RFA-NS-12-006, 1U01NS082320-01) and is supported by a Faculty Development Fellowship from the “Eleanor and Miles Shore 50th Anniversary Fellowship Program for Scholars in Medicine”, Boston Children’s Hospital, Department of Neurology, 2012–2013 and performs video-EEG long-term monitoring, EEGs, and other electrophysiological studies at Boston Children’s Hospital and bills for these procedures.

William Bosl receives funding from the Translational Research Project at Boston Children’s Hospital.

Alexander Rotenberg is funded by the NIH/NINDS, the Translational Research Project at Boston Children’s Hospital, the Center for Integration of Medicine & Innovative Technology (CIMIT) and also performs video-EEG long-term monitoring, EEGs, and other electrophysiological studies at Boston Children’s Hospital and bills for these procedures.

Tobias Lodenkemper serves on the Laboratory Accreditation Board for Long Term (Epilepsy and ICU) Monitoring (ABRET), on the American Board of Clinical Neurophysiology (ABCN), as Associate Editor for Seizure, the European Journal of Epilepsy, and on the Council of the American Clinical Neurophysiology Society (ACNS), performs video-EEG long-term monitoring, EEGs, and other electrophysiological studies at Boston Children’s Hospital and bills for these procedures, receives support from NIH/NINDS, is supported by a Career Development Fellowship Award from Harvard Medical School and Boston Children’s Hospital, by the Program for Quality and Safety at Boston Children’s Hospital, by the Payer Provider Quality Initiative, by the Translational Research Project at Boston Children’s Hospital, and receives funding from the Epilepsy Foundation of America (EF-213583 and EF-213882), the Epilepsy Therapy Project, the Pediatric Epilepsy Research Foundation, from the Center for Integration of Medicine & Innovative Technology (CIMIT), and from an investigator initiated grant from Lundbeck.

References

- [1] Lodenkemper T, Sánchez Fernández I, Peters JM. Continuous spike and waves during sleep and electrical status epilepticus in sleep. *J Clin Neurophysiol* 2011;28:154–64.
- [2] Nickels K, Wirrell E. Electrical status epilepticus in sleep. *Semin Pediatr Neurol* 2008;15:50–60.
- [3] Tassinari CA, Rubboli G, Volpi L, et al. Encephalopathy with electrical status epilepticus during slow sleep or ESES syndrome including the acquired aphasia. *Clin Neurophysiol* 2000;111(Suppl. 2):S94–S102.
- [4] Caraballo RH, Bongiorno L, Cersosimo R, Semprino M, Espeche A, Fejerman N. Epileptic encephalopathy with continuous spikes and waves during sleep in children with shunted hydrocephalus: a study of nine cases. *Epilepsia* 2008;49:1520–7.
- [5] Inutsuka M, Kobayashi K, Oka M, Hattori J, Ohtsuka Y. Treatment of epilepsy with electrical status epilepticus during slow sleep and its related disorders. *Brain Dev* 2006;28:281–6.
- [6] Liukkonen E, Kantola-Sorsa E, Paetau R, Gaily E, Peltola M, Granstrom ML. Long-term outcome of 32 children with encephalopathy with status epilepticus during sleep, or ESES syndrome. *Epilepsia* 2010;51:2023–32.
- [7] Nieuwenhuis L, Nicolai J. The pathophysiological mechanisms of cognitive and behavioral disturbances in children with Landau–Kleffner syndrome or epilepsy with continuous spike-and-waves during slow-wave sleep. *Seizure* 2006;15:249–58.
- [8] Robinson RO, Baird G, Robinson G, Simonoff E. Landau–Kleffner syndrome: course and correlates with outcome. *Dev Med Child Neurol* 2001;43:243–7.
- [9] Rossi PG, Parmeggiani A, Posar A, Scaduto MC, Chiodo S, Vatti G. Landau–Kleffner syndrome (LKS): long-term follow-up and links with electrical status epilepticus during sleep (ESES). *Brain Dev* 1999;21:90–8.
- [10] Sinclair DB, Snyder TJ. Corticosteroids for the treatment of Landau–Kleffner syndrome and continuous spike-wave discharge during sleep. *Pediatr Neurol* 2005;32:300–6.
- [11] Tassinari CA, Cantalupo G, Rios-Pohl L, Giustina E, Rubboli G. Encephalopathy with status epilepticus during slow sleep: “the Penelope syndrome”. *Epilepsia* 2009;50:4–8.
- [12] Akman CI. Nonconvulsive status epilepticus and continuous spike and slow wave of sleep in children. *Semin Pediatr Neurol* 2010;17:155–62.
- [13] Kaplan PW. No, some types of nonconvulsive status epilepticus cause little permanent neurologic sequelae (or: “the cure may be worse than the disease”). *Neurophysiol Clin* 2000;30:377–82.
- [14] Maganti R, Gerber P, Drees C, Chung S. Nonconvulsive status epilepticus. *Epilepsy Behav* 2008;12:572–86.
- [15] Thomas P. How urgent is the treatment of nonconvulsive status epilepticus? *Epilepsia* 2007;48(Suppl. 8):44–5.
- [16] Abend NS, Gutierrez-Colina A, Zhao H, et al. Interobserver reproducibility of electroencephalogram interpretation in critically ill children. *J Clin Neurophysiol* 2011;28:15–9.
- [17] Gerber PA, Chapman KE, Chung SS, et al. Interobserver agreement in the interpretation of EEG patterns in critically ill adults. *J Clin Neurophysiol* 2008;25:241–9.
- [18] Piccinelli P, Viri M, Zucca C, et al. Inter-rater reliability of the EEG reading in patients with childhood idiopathic epilepsy. *Epilepsy Res* 2005;66:195–8.
- [19] Webber WR, Litt B, Lesser RP, Fisher RS, Bankman I. Automatic EEG spike detection: what should the computer imitate? *Electroencephalogr Clin Neurophysiol* 1993;87:364–73.
- [20] Feldwisch-Drentrup H, Ihle M, Quyen Mle V, et al. Anticipating the unobserved: prediction of subclinical seizures. *Epilepsy Behav* 2011;22(Suppl. 1):S119–26.
- [21] Jouny CC, Franaszczuk PJ, Bergey GK. Improving early seizure detection. *Epilepsy Behav* 2011;22(Suppl. 1):S44–8.
- [22] Kharbouch A, Shoeb A, Guttig J, Cash SS. An algorithm for seizure onset detection using intracranial EEG. *Epilepsy Behav* 2011;22(Suppl. 1):S29–35.
- [23] Osorio I, Schachter S. Extracerebral detection of seizures: a new era in epileptology? *Epilepsy Behav* 2011;22(Suppl. 1):S82–7.
- [24] Raghunathan S, Jaitli A, Irazoqui PP. Multistage seizure detection techniques optimized for low-power hardware platforms. *Epilepsy Behav* 2011;22(Suppl. 1):S61–8.
- [25] Sackellares JC, Shiao DS, Halford JJ, LaRoche SM, Kelly KM. Quantitative EEG analysis for automated detection of nonconvulsive seizures in intensive care units. *Epilepsy Behav* 2011;22(Suppl. 1):S69–73.
- [26] Zandi AS, Dumont GA, Javidan M, Tafreshi R. Detection of epileptic seizures in scalp electroencephalogram: an automated real-time wavelet-based approach. *J Clin Neurophysiol* 2012;29:1–16.
- [27] Halford JJ. Computerized epileptiform transient detection in the scalp electroencephalogram: obstacles to progress and the example of computerized ECG interpretation. *Clin Neurophysiol* 2009;120:1909–15.
- [28] Wilson SB, Emerson R. Spike detection: a review and comparison of algorithms. *Clin Neurophysiol* 2002;113:1873–81.
- [29] Stevens JR, Lonsbury BL, Goel SL. Seizure occurrence and interspike interval. Telemetered electroencephalogram studies. *Arch Neurol* 1972;26:409–19.
- [30] Gotman J, Gloor P. Automatic recognition and quantification of interictal epileptic activity in the human scalp EEG. *Electroencephalogr Clin Neurophysiol* 1976;41:513–29.
- [31] Gotman J, Ives JR, Gloor P. Automatic recognition of inter-ictal epileptic activity in prolonged EEG recordings. *Electroencephalogr Clin Neurophysiol* 1979;46:510–20.
- [32] Kobayashi K, Watanabe Y, Inoue T, Oka M, Yoshinaga H, Ohtsuka Y. Scalp-recorded high-frequency oscillations in childhood sleep-induced electrical status epilepticus. *Epilepsia* 2010;51:2190–4.
- [33] Witte H, Eiselt M, Patakova I, et al. Use of discrete Hilbert transformation for automatic spike mapping: a methodological investigation. *Med Biol Eng Comput* 1991;29:242–8.
- [34] Webber WR, Litt B, Wilson K, Lesser RP. Practical detection of epileptiform discharges (EDs) in the EEG using an artificial neural network: a comparison of raw and parameterized EEG data. *Electroencephalogr Clin Neurophysiol* 1994;91:194–204.

- [35] Kalayci T, Ozdamar O. Wavelet preprocessing for automated neural network detection of EEG spikes. *IEEE Eng Med Biol* 1995;160–6 [March/April].
- [36] Indiradevi KP, Elias E, Sathidevi PS, Dinesh Nayak S, Radhakrishnan K. A multi-level wavelet approach for automatic detection of epileptic spikes in the electroencephalogram. *Comput Biol Med* 2008;38:805–16.
- [37] Zandi AS, Javidan M, Dumont GA, Tafreshi R. Automated real-time epileptic seizure detection in scalp EEG recordings using an algorithm based on wavelet packet transform. *IEEE Trans Biomed Eng* 2010;57:1639–51.
- [38] Argoud FI, De Azevedo FM, Neto JM, Grillo E. SADE3: an effective system for automated detection of epileptiform events in long-term EEG based on context information. *Med Biol Eng Comput* 2006;44:459–70.
- [39] Dümpelmann M, Elger CE. Visual and automatic investigation of epileptiform spikes in intracranial EEG recordings. *Epilepsia* 1999;40:275–85.
- [40] Adjouadi M, Cabrerizo M, Ayala M, et al. Detection of interictal spikes and artifactual data through orthogonal transformations. *J Clin Neurophysiol* 2005;22:53–64.
- [41] Larsson PG, Wilson J, Eeg-Olofsson O. A new method for quantification and assessment of epileptiform activity in EEG with special reference to focal nocturnal epileptiform activity. *Brain Topogr* 2009;22:52–9.
- [42] Nonclercq A, Foulon M, Verheulpen D, et al. Spike detection algorithm automatically adapted to individual patients applied to spike-and-wave percentage quantification. *Neurophysiol Clin* 2009;39:123–31.
- [43] De Lucia M, Fritschy J, Dayan P, Holder DS. A novel method for automated classification of epileptiform activity in the human electroencephalogram-based on independent component analysis. *Med Biol Eng Comput* 2008;46:263–72.
- [44] Aldenkamp AP, Arends J. Effects of epileptiform EEG discharges on cognitive function: is the concept of “transient cognitive impairment” still valid? *Epilepsy Behav* 2004;5(Suppl. 1):S25–34.
- [45] Dodrill CB. Neuropsychological effects of seizures. *Epilepsy Behav* 2004;5(Suppl. 1):S21–4.
- [46] Holmes G, Lenck-Santini P. Role of interictal epileptiform abnormalities in cognitive impairment. *Epilepsy Behav* 2006;8:504–15.
- [47] Majak K, Pitkanen A. Do seizures cause irreversible cognitive damage? Evidence from animal studies. *Epilepsy Behav* 2004;5(Suppl. 1):S35–44.
- [48] Nicolai J, Ebus S, Biemans DP, et al. The cognitive effects of interictal epileptiform EEG discharges and short nonconvulsive epileptic seizures. *Epilepsia* 2012;53:1051–9.
- [49] Bolsterli BK, Schmitt B, Bast T, et al. Impaired slow wave sleep downscaling in encephalopathy with status epilepticus during sleep (ESES). *Clin Neurophysiol* 2011;122:1779–87.
- [50] Diekelmann S, Born J. The memory function of sleep. *Nat Rev Neurosci* 2010;11:114–26.
- [51] Jordan KG. Neurophysiologic monitoring in the neuroscience intensive care unit. *Neurol Clin* 1995;13:579–626.